

U.S. Geological Survey public-access version of the following article:

Evaluation of Bias Associated with Capture Maps Derived from Nonlinear Groundwater Flow Models

By Cara Nadler¹, Kip Allander², Greg Pohl³, Eric Morway², Ramon Naranjo², and Justin Huntington³

Published in: *Groundwater*, Vol. 56, No. 3, May–June 2018, Page 458–469

Any use of trade, firm, or product names is for descriptive purposes only and does not imply endorsement by the U.S. Government

Although this information product, for the most part, is in the public domain, it also may contain copyrighted materials as noted in the text. Permission to reproduce copyrighted items must be secured from the copyright owner.

Include other disclaimer statements here, as appropriate. Author should refer to the FSP website for details.

USGS release date: December 2020

For link to publisher's version, see <https://pubs.er.usgs.gov/publication/70191177>.

¹Corresponding author: U.S. Geological Survey, 2730 N. Deer Run Road, Carson City, NV 89701; 775 887 7673; cnadler@usgs.gov

²U.S. Geological Survey, Carson City, NV 89701; kalland@usgs.gov; emorway@usgs.gov; rnaranjo@usgs.gov

³Desert Research Institute, Reno, NV 89512; greg.pohl@dri.edu; justin.huntington@dri.edu

Abstract

The impact of groundwater withdrawal on surface water is a concern of water users and water managers, particularly in the arid western United States. Capture maps are useful tools to spatially assess the impact of groundwater pumping on water sources (e.g., streamflow depletion) and are being used more frequently for conjunctive management of surface water and groundwater. Capture maps have been derived using linear groundwater flow models and rely on the principle of superposition to demonstrate the effects of pumping in various locations on resources of interest. However, nonlinear models are often necessary to simulate head-dependent boundary conditions and unconfined aquifers. Capture maps developed using nonlinear models with the principle of superposition may over- or underestimate capture magnitude and spatial extent. This paper presents new methods for generating capture difference maps, which assess spatial effects of model nonlinearity on capture fraction sensitivity to pumping rate, and for calculating the bias associated with capture maps. The sensitivity of capture map bias to selected parameters related to model design and conceptualization for the arid western United States is explored. This study finds that the simulation of stream continuity, pumping rates, stream incision, well proximity to capture sources, aquifer hydraulic conductivity, and groundwater evapotranspiration extinction depth substantially affect capture map bias. Capture difference maps demonstrate that regions with large capture fraction differences are indicative of greater potential capture map bias. Understanding both spatial and temporal bias in capture maps derived from nonlinear groundwater flow models improves their utility and defensibility as conjunctive-use management tools.

Introduction

Capture, as first described by Theis (1940), is the change in inflow to or outflow from a groundwater system caused by groundwater pumping. Numerous studies have revisited and expanded upon the concept of capture (Bredehoeft et al. 1982; Leake et al. 2008; Leake et al. 2010; Barlow and Leake 2012; Davids and Mehl 2014; Konikow and Leake 2014). At the onset of pumping, water is removed from storage as drawdown surrounding the well (the cone of depression) extends outward. This drawdown and depletion of stored water continues until the hydraulic gradient between the well and a source of recharge and/or discharge changes. This change allows the pumping to intercept or “capture” a flow of water eventually equal to the pumping rate (Theis 1940; Barlow and Leake 2012). Groundwater captured by a pumping well may come from multiple sources (capture sources), such as streamflow depletion and salvaged groundwater evapotranspiration (ET_g). Streamflow depletion as a source of capture is the combination of induced seepage from streams to the groundwater system and decreased discharge from the groundwater system to streams. Salvaged ET_g as a source of capture is the diversion of water to a pumping well that would otherwise have naturally discharged via ET_g. Capture can be described in volumetric terms (volumetric capture rate), or it can be expressed as a fraction of capture rate, either instantaneous or cumulative, to the pumping rate causing the change (capture fraction) and is often determined through use of groundwater flow models (Leake et al. 2010). Capture fractions, once calculated at numerous points in a system through time, can be contoured to produce a capture map as a visual aid to describe spatial variations in the relative amount of stream capture in response to groundwater pumping for a particular time (Cosgrove and Johnson 2005; Leake et al. 2008; Peterson et al. 2008; Leake et al. 2010; Stanton et al. 2010). Capture maps provide spatiotemporal information on how a new or existing well affects some source of capture in an easily interpreted format. Capture map methods can be automated, thus requiring minimal extra work to generate such a visually informative tool. The methods used in this paper to develop capture maps are described by Leake et al. (2010).

The use of capture maps to predict the combined effect of multiple pumping wells on stream capture relies on the principle of superposition. However, the principle of superposition is only applicable for linear groundwater flow models (Reilly et al. 1987), and not necessarily appropriate for nonlinear models, which are needed to simulate head-dependent flow processes (i.e., ET_g, drying streams) and unconfined aquifers (Konikow 2014). Thus, when using a capture map derived from a nonlinear groundwater flow model to estimate capture for multiple wells, use of the principle of superposition may bias results and lead to an erroneous estimate of “true” capture. For example, capture map analyses are generally developed with linear models by inserting a pumping well in a model one cell at a time and comparing the model results to the same model but without the pumping stress. Model results from each individual model run (corresponding to each new well) are presented as a single mosaic known as a capture map. The volumetric capture rate calculated from each individual model run is added together (i.e., the principle of superposition is applied) with the capture map methods. Such methods may be used to determine the cumulative impact of an actual or hypothetical well distribution on a source of capture, such as a stream or stream reach. As will be shown, the total capture calculated in this way vs. the total capture that is calculated when pumping the same set

of wells simultaneously may be different when determined using a nonlinear model. This difference, hereafter referred to as “capture map bias,” describes the tendency of a capture map to either over- or underestimate “true” capture. The predictive accuracy of a capture map derived from a nonlinear model is not well understood where capture map bias is significant.

The purpose of this study is to quantify and analyze bias associated with capture maps derived from nonlinear groundwater flow models in order to enhance capture map development and interpretation. A novel approach for calculating capture map bias is presented. A hypothetical stream-aquifer system model is used to generate capture maps and capture difference maps, which assess the degree of model nonlinearity through space and time with respect to pumping rate. Capture difference maps are useful for identifying regions of significant capture bias through time. The value of capture difference maps in identifying capture map bias is then tested with a capture bias analysis in two separate regions of interest. In addition, the study explores the sensitivity of the capture bias associated with various model parameters (e.g., hydraulic conductivity, pumping rate) using a hypothetical model of a typical stream-aquifer system in the arid western United

Methods

The method used to compute capture fractions and generate capture maps using a groundwater flow model have been discussed by Leake et al. (2010); however, new methodology and terminology are presented to further explore difficulties associated with applying the principle of superposition to nonlinear models:

- *Capture Difference Map*, is a map derived from subtracting one capture map developed using a high pumping rate from another developed using a low pumping rate.
- *Capture Map Bias*, is defined as the over- or underestimation of capture using capture maps derived from nonlinear groundwater flow models. Bias in pumping-induced storage depletion also is included here.
- *Capture Map Derived Capture (CMDC)*, is defined as capture determined for a select group of wells using capture map methods developed by Leake et al. (2010).

Capture Maps and Capture Difference Maps: Hypothetical Stream-Aquifer System

A nonlinear groundwater flow model of a hypothetical, unconfined, stream-aquifer system was created to characterize capture bias resulting from variations in model design and conceptualization (Figure 1 and Table 1). The model is represented by one layer that is between 100 and 130 feet thick with 30 rows and 100 columns (3000 cells). The model includes a stream, one source of recharge other than from streams (i.e., mountain block recharge), ETg permitted across the entire model domain, and six pumping wells. Aquifer and streambed hydraulic properties were specified at 1 ft/d. In the hypothetical system, ETg is simulated with the MODFLOW Evapotranspiration (EVT) Package (Harbaugh 2005), mountain block recharge is simulated with the MODFLOW Recharge (RCH) Package (Harbaugh 2005), and the stream is either simulated with the MODFLOW Time-Variant Specified-Head (CHD) Package (Harbaugh 2005) or the Streamflow-Routing (SFR) Package (Niswonger and Prudic 2005). Both the EVT and SFR Packages simulate head-dependent boundary conditions that allow ETg and streamflow to vary with the simulated position of the water table. Predevelopment depth to water ranges from approximately 8 feet along the stream boundary to approximately 30 feet along the no-flow boundary parallel to the river. As much as 30 feet of drawdown occurs after 200 years of pumping in some locations (Figure 1B). Groundwater flow for this hypothetical stream-aquifer system is simulated using MODFLOW-NWT (Niswonger et al. 2011). MODFLOW-NWT is well-suited for simulating unconfined aquifers and other non-linear boundary conditions by keeping dewatered cells active and applying an upstream weighting function to smooth cell connections in the discretized groundwater-flow equation.

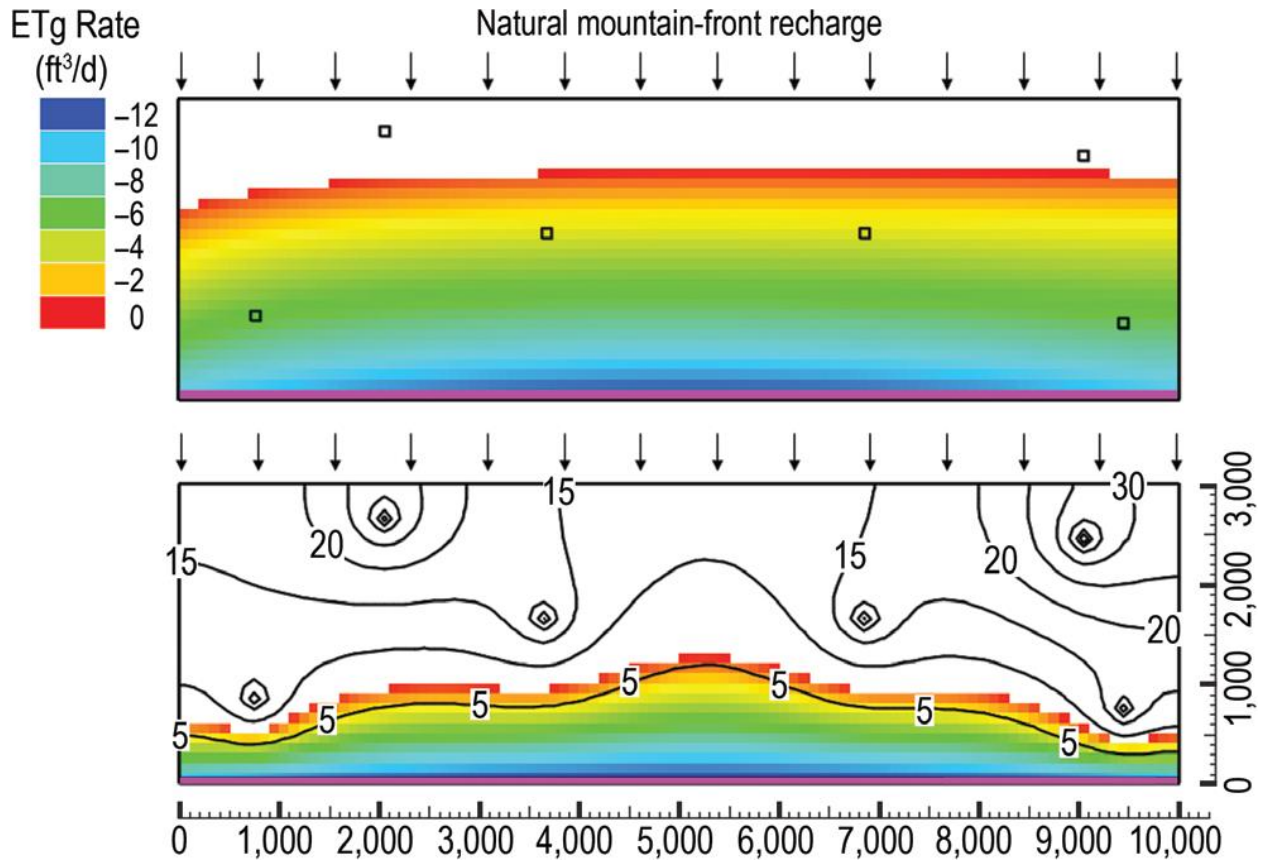


Figure 1. Plan view of hypothetical stream-aquifer system with a stream shown in purple, wells indicated by black boxes, and the position of mountain block recharge indicated by arrows. The hypothetical system is 10,000 feet by 3000 feet with ground elevation varying between 130 feet in the upper left corner and 100 feet in the lower right corner. The color grid represents ETg distribution in predevelopment conditions (A) and after 200 years of pumping six wells (B). A linear ETg rate can be derived by dividing the presented value by the cell surface area (10,000 ft²). Drawdown after 200 years of pumping six wells simultaneously at 2500 ft³/d is contoured in black (B).

Table 1. Model Parameters for Hypothetical Stream-Aquifer System and the Parameters Listed Below Detail the Reference Model

Parameter	Value
Streambed K	1 ft/d
Stream inflow	25,000 ft ³ /d
Stream incision	10 ft
Aquifer K	1 ft/d
Specific yield	0.2
Layers	1
Maximum ETg rate	0.002 ft/d
ETg extinction depth	20 ft
Grid discretization	100 feet × 100 feet
Pumping rate	2500 ft ³ /d per well
Recharge	0.004 ft/d

Capture maps for the hypothetical stream-aquifer system are produced for five different pumping rates: 250 ft³/d, 750 ft³/d, 1250 ft³/d, 1900 ft³/d, and 2500 ft³/d (7 m³/d, 21 m³/d, 35 m³/d, 54 m³/d, and 71 m³/d) using the methods described by Leake et al. (2010). Capture maps are developed by contouring capture fractions for a well pumping individually in each of the 3000 model grid cells. Capture fractions used to create capture maps derived from linear

groundwater flow models can be applied as a percentage of capture to any proposed pumping rates; however, capture fractions associated with nonlinear groundwater flow models are most appropriately applied to pumping rates similar to those used to calculate the fraction. Thus, regions in which capture fractions substantially vary when derived from different pumping rates are indicative of model nonlinearity. Capture map utility is limited in regions affected by increasing model nonlinearity.

Capture difference maps are created to assess spatiotemporal change in capture fractions caused by varying simulated pumping rates using methods similar to those described by Stanton et al. (2010). Capture difference maps are made by subtracting the capture fraction array generated by the higher pumping rate from the capture fraction array generated by the lower pumping rate. The resulting difference between two capture fractions caused by two different pumping rates is plotted for each grid cell and contoured. Negative differences indicate a higher capture fraction from a higher pumping rate as compared with a lower pumping rate, whereas positive values indicate a lower capture fraction from a higher pumping rate as compared with a lower pumping rate. Linear behavior with respect to pumping rate is indicated by zero or near zero capture difference and indicate regions in which capture fractions are independent of pumping rate. Regions where capture differences are insignificant for a given model (perhaps varying by less than 10%) are regions where the capture maps are resilient and generally can be used effectively for managing capture from groundwater pumping. Capture difference maps were developed for salvaged ETg, streamflow depletion, and storage depletion after 30 years of pumping (once the system has become nearly capture-dependent) for the hypothetical stream-aquifer system.

Capture Bias and Parameter Sensitivity Analysis

The first step in assessing capture bias is to run the hypothetical model with a steady-state stress period without pumping. Reference values are obtained from the steady-state run that are used for the computation of groundwater storage and capture components of interest (i.e., streamflow depletion, salvaged ETg). Although the capture analysis presented in this paper uses steady state models for water budget reference values, capture also can be calculated using a consistent transient stress field over time as reference. Six wells were then chosen for the bias analysis to conceptually represent a hypothetical pumping distribution. The hypothetical model is then run with a transient stress period with one well pumping at a time. An individual model run is required for each well in the distribution so that capture and depletion rates may be calculated individually over time for all of the wells. The individual capture rates derived for each pumping well are added (superposed) to produce CMDC which represents the total capture for the selected distribution of wells as derived from a capture map. Actual capture is determined by simulating the same group of wells pumping simultaneously and calculating the resulting capture over time. Capture map bias is computed by comparing CMDC and actual capture using the equation:

$$\text{CaptureMapBias (\%)} = \frac{\text{CMDC} - \text{Actual Capture}}{|Q_p|} * 100$$

where Q_p = pumping rate.

This analysis is carried out with CMDC and actual capture represented as volumetric rates. The same methods are applied to storage depletion. The capture map bias analysis is applied to a new well distribution placed in two regions of the hypothetical model domain. The capture map bias of the two regions is used to test the relationship between capture difference maps and capture bias. First, capture bias is computed for a scenario using six pumping wells placed in a region with high streamflow depletion capture fraction differences. Next, capture bias is computed for a scenario using six pumping wells placed in a region of minimal capture fraction differences. Capture bias is expected to be greater with the wells placed in a region of greater capture fraction differences.

The location and magnitude of capture map bias was investigated with a series of sensitivity analyses. The sensitivity analyses adjust model conceptualization and parameters typically found in the arid western United States. Stream representation was assessed by simulating a plentiful stream first with the MODFLOW Time-Varying Specified-Head (CHD) Package (Harbaugh et al. 2000) and then with the MODFLOW Streamflow- Routing (SFR) Package (Niswonger and Prudic 2005). The MODFLOW CHD Package is a specified head boundary that supplies the required amount of water to a cell in order to maintain the specified head. The MODFLOW SFR Package is a head-dependent boundary in which base flow and streamflow depletion change with the position of the water table relative to stream stage. The MODFLOW SFR Package is used for all other modeling of the hypothetical aquifer and parameters specified in this package (streambed hydraulic conductivity, stream inflow rate, streambed elevation)

are varied to characterize capture map bias sensitivity. Stream inflow rate is used to evaluate bias sensitivity to stream continuity. Stream inflow was reduced to allow 0%, 53%, and 83% of stream reaches to go dry. Streambed elevation was used to represent the relationship between bias and stream incision (model top elevation minus streambed elevation).

Sensitivity of capture bias to ET_g representation was assessed with two parameters. The MODFLOW EVT Package is a head-dependent boundary condition in which the specified maximum ET_g rate occurs when the water table is at the specified ET_g surface elevation (land surface in this case), and the ET_g rate linearly decreases to zero as the water table lowers to the specified extinction depth. The maximum ET_g rate and extinction depth are varied for the sensitivity analysis. The sensitivity analysis also evaluated parameters used in model design and conceptualization. Aquifer hydraulic conductivity (*K*) and specific yield were varied to assess bias sensitivity to aquifer properties in the presence of nonlinear flow processes. Pumping rate, well location, and grid discretization were also evaluated. The number of layers was also assessed with a three-layer model that included an unconfined top layer, a less permeable middle layer, and a more permeable bottom layer. Wells were simulated to pump from the bottom layer and capture map bias results were compared to a one-layer, unconfined model with the same well distribution in the horizontal plane. As results were nearly the same, all other evaluations were done for a single, unconfined layer.

One parameter was varied at a time for each model run in the sensitivity analyses and each analysis includes the parameter values found in the reference model (Table 1). Capture map bias was computed for each variation of the hypothetical stream-aquifer system model and the greatest occurrence of capture map bias for each variation was reported. Parameter variations and associated capture map biases can be found in Table 2 in the Results and Discussion section below. Capture map bias sensitivity is calculated by taking the greatest difference in the maximum capture bias between two models with one varied parameter across the entire model simulation period. Large differences in the maximum occurrence of capture map bias, regardless of time, indicate greater sensitivity to a given parameter. Although efforts were made to explore capture bias sensitivity to all important parameters suspected of influencing capture bias, other untested parameters also may affect capture bias behavior. Users of these methods are encouraged to further characterize capture bias when assessing models that have other forms of capture or different sources of model nonlinearity.

Table 2
Model Parameter Variations for Hypothetical Stream-Aquifer System with Associated Greatest Magnitude Capture Map Biases

Parameter	Values	Bias		
		Streamflow Depletion (%)	Salvaged ETg (%)	Storage Depletion (%)
Specific yield (dimensionless)	0.02	-13.1	13.6	-6.6
	0.1	-13.1	14.0	-8.1
	0.2 ¹	-13.1	14.0	-8.3
	0.3	-13.1	14.0	-8.4
Streambed K (ft/d)	0.1	-13.0	14.3	-8.7
	1 ¹	-13.1	14.0	-8.3
	10	-13.1	14.0	-8.3
Grid discretization (ft × ft)	20 × 20	-13.4	14.5	-8.7
	50 × 50	-13.6	14.5	-8.8
	100 × 100 ¹	-13.1	14.0	-8.3
Maximum ETg rate (ft/d)	0.001	-12.5	12.8	-7.4
	0.002 ¹	-13.1	14.0	-8.3
	0.003	-12.9	14.2	-8.6
	0.004	-12.5	14.1	-8.6
CHD vs. SFR	CHD	-14.5	15.2	-8.6
	SFR ¹	-13.1	14.0	-8.3
Layers	1 ¹	-13.1	14.0	-8.3
	3	-11.0	12.5	-8.8
Stream continuity ² (% dry reaches)	0 ¹	-13.1	14.0	-8.3
	7	-10.7	14.0	-8.4
	18	-5.7	13.5	-8.6
Pumping rate (ft ³ /d)	250	-0.4	0.7	-0.6
	1250	-4.1	5.0	-4.0
	2500 ¹	-13.1	14.0	-8.3
Stream incision (ft)	2.5	-6.9	8.5	-6.2
	5	-8.7	10.1	-7.0
	10 ¹	-13.1	14.0	-8.3
	15	-18.6	18.8	-9.1
	20	-23.5	23.6	-8.7
Well proximity (distance from stream/riparian zone, ft)	500	-0.1	0.3	-0.2
	1200	-11.3	12.1	-7.6
	1900	-17.8	19.1	-12.0
	2600	-19.4	21.1	-14.0
Aquifer K (ft/d)	0.75	-16.4	17.5	-10.6
	1 ¹	-13.1	14.0	-8.3
	5	-1.7	1.7	-1.0
	10	4.8	-4.8	-3.1
ETg extinction depth (ft)	5	2.0	0.0	-2.0
	10	-25.9	26.0	-8.8
	15	-18.2	18.5	-8.9
	20 ¹	-13.1	14.0	-8.3
	25	-9.3	10.5	-7.2
	Average	-11.7	12.8	-7.6
	Max	4.8	26.0	-0.2
	Min	-25.9	-4.8	-14.0
	Standard Deviation	0.061	0.060	0.027

Notes: CHD describes a stream represented with the MODFLOW Time-Variant Specified-Head Package and SFR describes a stream represented with the MODFLOW Streamflow-Routing Package.

¹The reference model parameters, as described in Table 1.

²Stream inflow is the parameter used to derive stream continuity in this paper. Other parameters may be varied to result in dry reaches (i.e., aquifer K, ETg rate).

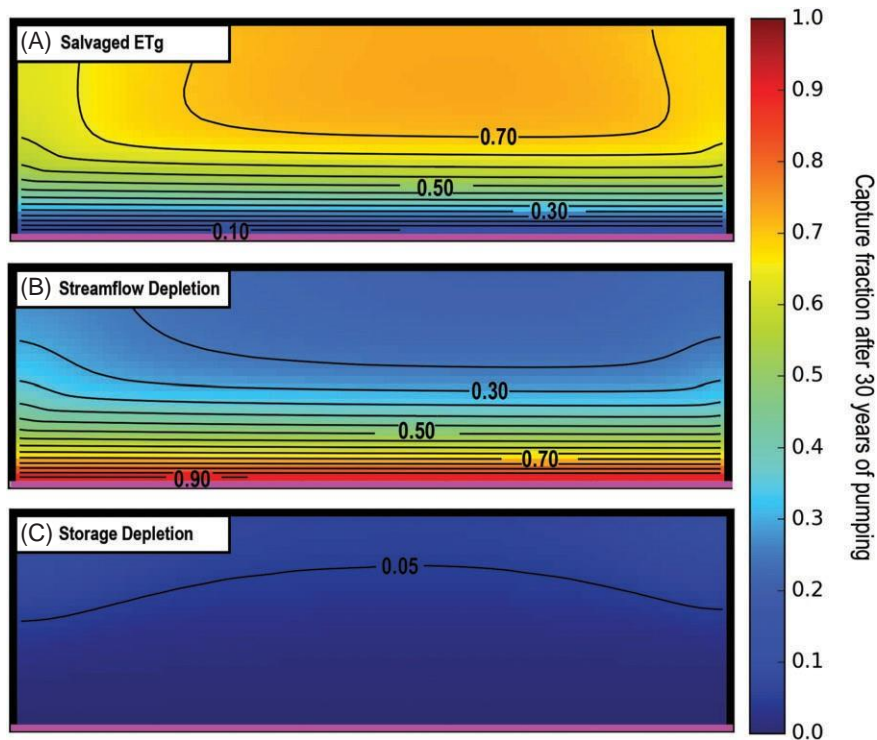


Figure 2. Capture maps for (A) salvaged ETg, (B) streamflow depletion and (C) groundwater storage depletion after 30 years of pumping at 1250 ft³/d. No-flow boundaries are shown with thick black lines. The location of the stream is shown in purple. Low capture fractions are shown in dark blue and high capture fractions are shown in red. The system represented has become capture-dependent with groundwater storage no longer a major source of water for the wells (contour line represents a value of 0.05). Near the stream/riparian zone the wells are relying more heavily on streamflow depletion. As wells are placed farther and farther from the stream/riparian zone, salvaged ETg becomes the major source of capture.

Results and Discussion

Capture Maps

Capture maps for salvaged ETg and streamflow depletion, and storage depletion maps depict a nearly 100% capture-dependent system after 30 years of pumping for all pumping rates tested (250 ft³/d, 750 ft³/d, 1250 ft³/d, 1900 ft³/d, and 2500 ft³/d or 7 m³/d, 21 m³/d, 35 m³/d, 54 m³/d, and 71 m³/d). The capture maps for all of the pumping rates are visually similar so only maps associated with the median pumping rate of 1250 ft³/d (35 m³/d) are shown in Figure 2. As expected, streamflow depletion decreases with distance from the stream and salvaged ETg increases with distance from the stream. Fractions derived from capture and depletion maps developed for each pumping rate after 30 years of pumping indicate a strong, nearly linear relation with pumping magnitude (Figure 3 and top right of Figure 4). The slope of the lines in Figure 3 is a result of the model being nonlinear. Capture fractions in linear models are independent of pumping rate and result in no change in capture fractions with changing pumping rate.

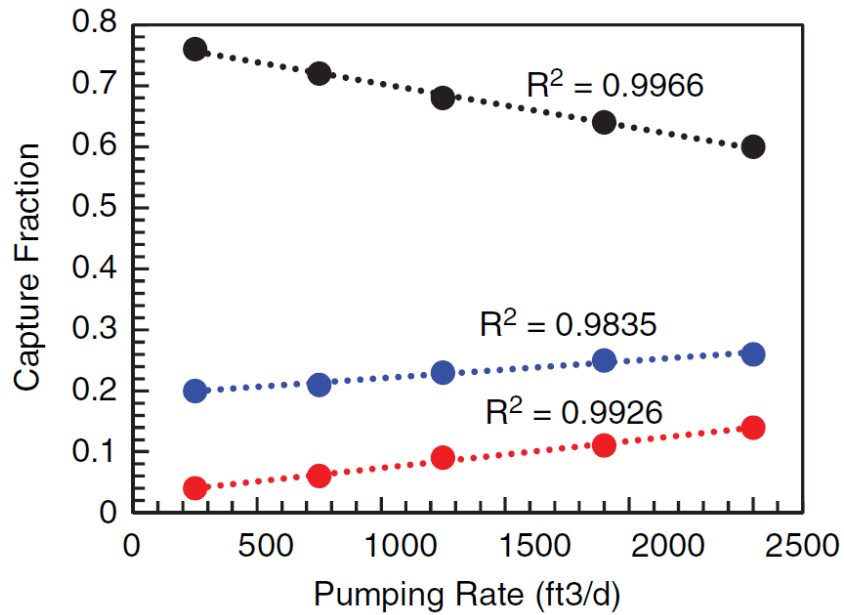


Figure 3. Capture fractions based on instantaneous volumetric rates derived from a range of pumping rates for one particular location (see Figure 4) after 30 years of pumping. Salvaged ETg (black), streamflow depletion (blue), and storage depletion (red) capture fractions demonstrate strong relationships with pumping rate.

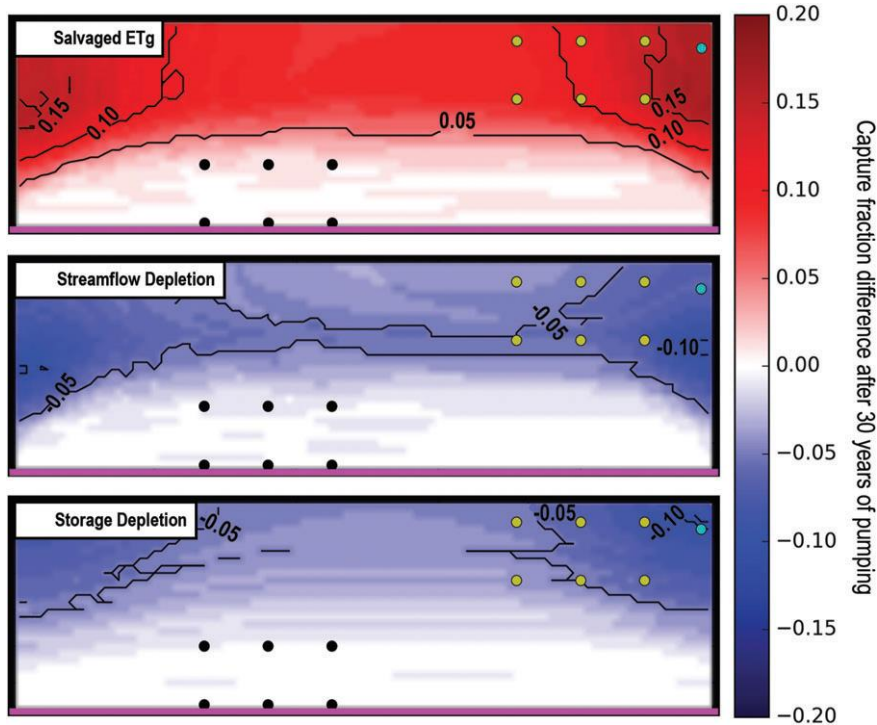


Figure 4. Capture difference maps for (A) salvaged ETg, (B) streamflow depletion and (C) groundwater storage depletion after 30 years of pumping. No-flow boundaries are shown with thick black lines. The location of the stream is shown in purple. Capture fraction differences are calculated by subtracting the capture fraction for a pumping rate of 2500 ft³/d from the capture fraction for a pumping rate of 250 ft³/d. The location used to compare pumping rates to associated capture fractions for Figure 3 is shown with a cyan circle in the upper right corner. Well locations used to calculate

capture map bias for Figure 5 are shown in black circles for a location of low capture fraction differences and in yellow circles for a location of high capture fraction differences.

Capture Difference Maps

Capture and depletion difference maps are created by differencing capture maps derived from two different pumping rates. Capture difference maps generally demonstrate consistent regions of differences that change linearly with magnitude of difference in pumping rates used to derive them. Thus, only a single difference map needs to be evaluated. A capture difference map developed by differencing capture maps derived from the lowest and highest reasonable pumping rates is optimal for understanding the greatest potential spatiotemporal capture map bias. Figure 4 shows the capture difference between the maximum and minimum pumping rates (250 ft³/d and 2500 ft³/d) after 30 years of pumping. These maps show the distributions of capture and depletion differences for salvaged ETg, streamflow depletion, and storage depletion. Red regions demonstrate positive differences which indicate capture fractions derived from lower pumping rates are greater than capture fractions derived from higher pumping rates. Blue regions demonstrate negative differences which indicate capture fractions derived from lower pumping rates are lower than capture fractions derived from higher pumping rates. White and near-white regions demonstrate zero and near-zero differences, indicating capture fractions are generally independent of pumping rates. The capture difference maps clearly show that capture and depletion fraction differences for all three sources of water to a well are least near the river boundary, and greatest in the corners of the model domain away from the river. The average capture fraction and depletion fraction difference are 0.07, 0.03, and 0.03 for salvaged ETg, streamflow depletion, and storage depletion, respectively. Though capture and depletion fraction differences between 250 ft³/d and 2500 ft³/d are relatively minor, it is clear that capture and depletion fraction differences vary spatially and temporally. The greatest difference in capture and depletion fractions shown on the maps in Figure 4 for salvaged ETg, streamflow depletion, and storage depletion are 0.17, -0.10, and -0.10, respectively. Regions with greater capture and depletion fraction differences are indicative of greater potential capture and depletion map bias.

Positive capture fraction differences in ETg (Figure 4A, red) indicate that lower pumping rates result in higher relative capture than do higher pumping rates. ETg is the only capture component that exhibits this behavior. Wells pumping at the lower rate derive a greater proportion of their water from salvaged ETg than the wells pumping at the higher rate. At higher pumping rates, the water table is lowered faster than at lower pumping rates. As a result, higher pumping rates increase gradients to stream boundaries sooner and therefore source a greater proportion of water from streamflow depletion sooner.

Conversely, negative capture and depletion fraction differences indicate that lower pumping rates result in lower capture and depletion fractions than higher pumping rates for streamflow (Figure 4B, blue) and groundwater storage (Figure 4C, blue). Capture fraction differences for streamflow depletion increase in magnitude away from the stream. Similar to salvaged ETg capture fractions, wells pumping at higher rates far from the stream are able to lower the water table faster, and induce seepage from the stream sooner. Because higher pumping rates result in smaller area available to capture ETg, a greater quantity is supplied by streamflow depletion.

Capture map bias is compared for a fixed arrangement of six wells in a region with greatest capture differences (top right; Figure 4) and in a region of lowest capture difference (bottom center; Figure 4). As expected, the capture bias is greater in the region of greater capture fraction differences than in the region with lower capture fraction differences (Figure 5). For the wells placed in an area of greatest capture fraction differences, captured salvaged ETg is overestimated by a maximum of 26%, and captured streamflow and storage depletion are underestimated by maximums of 22% and 18%, respectively. Conversely, for the wells placed in the area of lowest capture fraction differences, capture and depletion were under- or overestimated by 2% to 3% for each source of water to a well. Based on this analysis, capture and depletion fraction differences and capture and depletion map biases show a positive correlation. This positive correlation demonstrates that difference maps are useful indicators of bias in space and time, making them valuable tools for a cursory initial assessment of the potential bias associated with capture maps developed from nonlinear groundwater flow models. Capture difference maps may be useful for limiting the spatial extent of capture maps to reduce associated potential bias. Where capture difference values are small, say less than 0.1, then capture map bias is likely insignificant. Regions with capture fraction differences greater than a predetermined bias threshold may be clipped from associated capture maps to improve capture map accuracy. A predetermined bias threshold may be used to define regions of applicability or conversely regions with limited applicability.

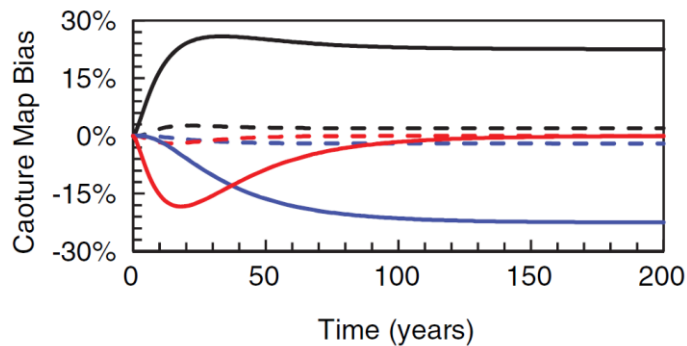


Figure 5. Changes in capture bias over time. Solid lines represent capture bias results for six wells placed in an area of high capture fraction differences (yellow circles in Figure 4) whereas dashed lines represent capture bias results for six wells placed in an area of low capture fraction differences (black circles in Figure 4). Salvaged ETg bias is shown in black, streamflow depletion bias is shown in blue, and storage depletion bias is shown in red.

Capture Bias

Generally, streamflow depletion and storage depletion bias are negative (underestimating capture and depletion) whereas salvaged ETg bias tends to be positive (overestimating capture) (Figure 5). When compared to predevelopment (i.e., steady-state) conditions, bias is essentially zero at the start of pumping and increases in magnitude over time. Generally, storage depletion bias is negative, grows in magnitude, then returns to zero once the system has reached a new state of equilibrium. Once storage depletion bias returns to zero, capture biases equilibrate as the system becomes 100% capture-dependent.

Capture map bias is the result of the model nonlinearity associated with simulating an unconfined aquifer with a head-dependent boundary condition that becomes spatially limited over time via a declining water table. The nonlinearity of the system allows capture values to vary with different instantaneous pumping rates. As a result, the combined influence of each of the individual pumping wells (CMDC) on a head-dependent boundary condition may be greater or less than the influence of all pumping wells when pumped simultaneously. Positive capture map bias indicates that actual capture for a given distribution of pumping wells is overestimated with capture map methods. When the given distribution of well pumps together to obtain actual capture, the unconfined groundwater system experiences greater drawdown more rapidly than the cumulative effect of individual pumping used to derive CMDC. The temporal offset in drawdown between these methods causes the model to result in different transmissivity values for methods used to derive CMDC and actual capture. Thus, the higher instantaneous pumping rates used to derive actual capture lower the water table in areas of ETg more rapidly and due to extinction depth, effectively shrink the area available to salvage ETg via nonlinear processes.

Negative capture map bias indicates that actual capture for a given distribution of pumping wells is underestimated with capture map methods. Like salvaged ETg bias, streamflow depletion bias is affected by the temporal offset in drawdown between CMDC and actual capture methods, which causes the model to result in different transmissivity values for each method used. Although the stream is not spatially limited by pumping (defined by having dry reaches) when a sufficient stream inflow rate is specified, the model design still allows the spatial distribution of ETg to reduce over time with the declining water table. Actual capture of ETg is overestimated because the spatial extent of ETg is not sufficiently reduced using capture map methods. This results in an underestimation of streamflow depletion and storage depletion using capture map methods with a nonlinear model. Thus unlike salvaged ETg, streamflow depletion bias is negative as the greater drawdown caused by actual pumping of the wells simultaneously causes faster drawdown in the system without reducing the spatial extent of the simulated stream (head-dependent boundary condition). The cumulative effect of individually pumped wells (CMDC) takes longer to cause the same drawdown in the nonlinear system than the simultaneous effect of the same wells pumping together. Thus, CMDC is less than actual capture for a connected stream. This relationship is altered when the inflow rate is reduced, allowing the stream to go dry. In this case, streamflow depletion bias becomes less negative and under the right conditions can become positive, transitioning from underestimation to overestimation. The higher pumping rates used to derive actual capture lower the water table along the stream more rapidly and due to the stream

connection to the aquifer, effectively shrink the area available to capture water from the stream represented as a head-dependent boundary.

Sensitivity of Capture Map Bias to Model Parameters and Stream Boundary Representation

Capture bias is variably sensitive to different model parameters and representation of head-dependent boundary types. Capture bias sensitivity is a function of model nonlinearity and is largely affected by changes in drawdown and aquifer diffusivity. Figure 6 shows the greatest capture bias sensitivity to each evaluated parameter for each capture and depletion component using values presented in Table 2. Generally, capture bias is most sensitive to the extinction depth of ET_g, aquifer hydraulic conductivity, well proximity to a stream, model representation of stream incision, pumping rates, and stream continuity. Capture bias appears to be much less sensitive to specific yield, streambed hydraulic conductivity, maximum rate of ET_g at surface, horizontal grid discretization, representation of a stream as a specified head boundary (MODFLOW CHD) or SFR, and number of model layers.

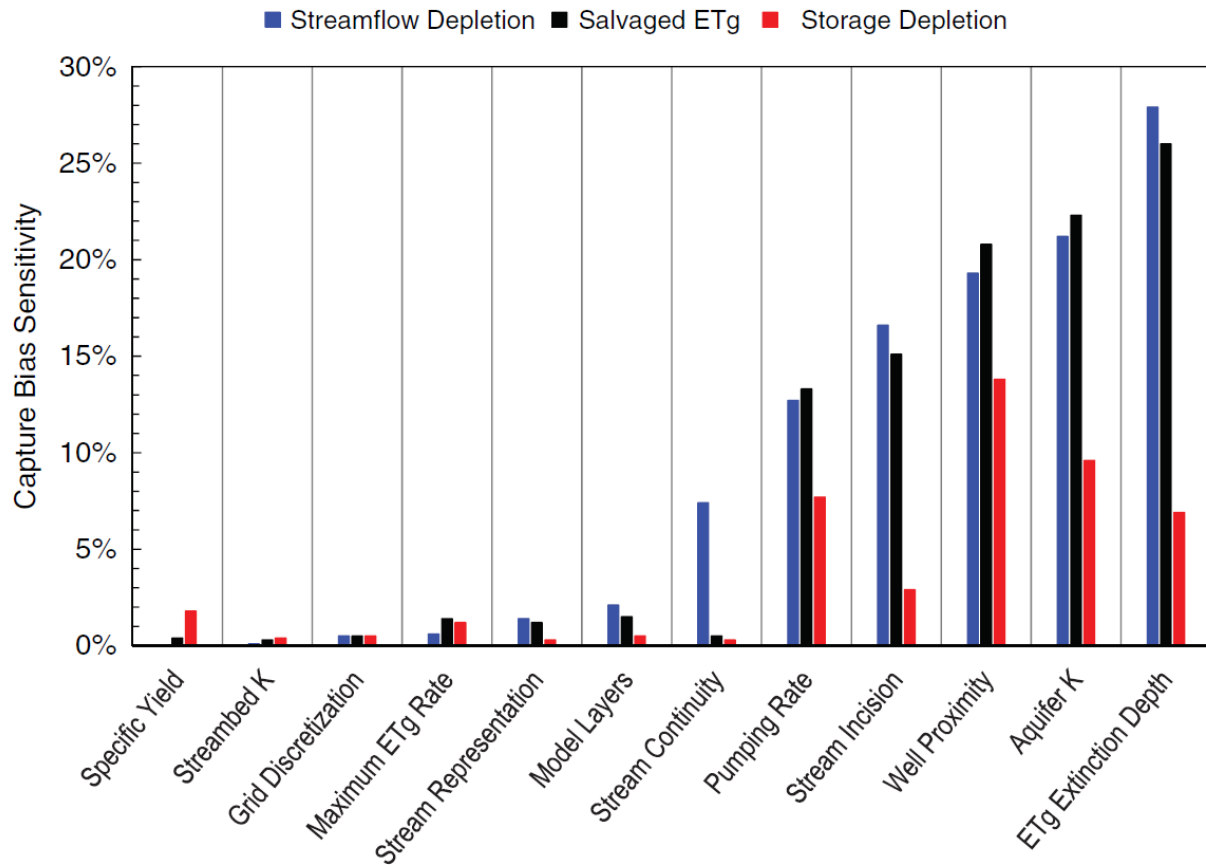


Figure 6. Capture map bias sensitivity for selected model parameters. Capture bias sensitivity equals the maximum difference in the greatest occurrence of capture map bias caused by varying a model parameter over the range of values shown in Table 2. The maximum difference between greatest occurrences of capture map bias is considered a surrogate for the sensitivity of capture map bias to a given parameter.

Model parameter variations that affect simulated ET_g (i.e., lower or raise the water table) can significantly increase capture map bias. Head-dependent boundary conditions, such as ET_g, allow volumetric capture rate to decrease to zero in some model cells with a decreasing water table. The spatial variability of the cells with capture rates that have reduced to zero stress the difference, or bias, of CMDC. When pumping wells cause enough drawdown to decrease the spatial extent of ET_g as a function of extinction depth, salvaged ET_g capture derived from capture maps tends to be overestimated. A shallow ET_g extinction depth causes a more nonlinear response to pumping because of a larger volumetric change in ET_g capture per unit change in simulated water level. As a result, shallow ET_g extinction depths are more sensitive to smaller water level fluctuations and typically are associated with greater

capture bias. Conversely, the maximum ETg rate does not increase the nonlinear response to pumping because the ETg rate decreases linearly with a water table between the ETg surface and extinction depth. Stream incision, as specified with a streambed elevation relative to the model surface, also has an important influence on capture bias. In particular, capture bias is very sensitive to stream incision when depth of stream incision approaches the ETg extinction depth. Small changes in simulated water levels can contribute greatly to model nonlinearities if stream incision and ETg extinction depth are similar.

Capture bias is generally sensitive to variations in model parameters that affect the simulated position of the water table. Such changes in turn influence groundwater surface-water interactions. In general, streamflow depletion is underestimated when derived from capture maps. However, this trend is generally reversed when streams are not continuous and go dry (stream continuity; Figure 6). Stream discontinuity could be caused by stream inflow rates that are insufficient to supply the stream losses incurred along the full length of the stream, increased pumping, or increased aquifer hydraulic conductivities that allow for more rapid streamflow depletion. At times this shift in capture map bias can result in substantial reduction in negative bias to near zero or even result in positive bias. This results from the model nonlinearity associated with the unconfined aquifer coupled with the nonlinear spatial variations in the stream (i.e., dry reaches). The simultaneous pumping (used to derive actual capture) causes greater drawdown than the cumulative effect of individual pumping (used to derive CMDC). As a result, actual pumping causes streamflow depletion sufficient to dry stream reaches sooner than experienced from the combined influence of individual wells pumping (CMDC). Thus, the streamflow depletion derived from capture maps for a discontinuous stream for a given well distribution is often overestimated with respect to nonlinear models.

The magnitude of capture bias is largely influenced by head-dependent boundary conditions (as represented by the MODFLOW SFR and EVT Packages) used to simulate capture sources that may contribute varying inflow into the model depending on model design and conceptualization. Such varying inflow may result from a combination of large pumping rates and aquifer hydraulic conductivities; shallow ETg extinction depths in the presence of deep stream incisions; or discontinuous streams. Capture map bias is greatest when head-dependent boundary conditions are most influenced by pumping magnitudes that decrease the spatial extent of the represented boundary condition. Capture bias generally increases with decreasing aquifer hydraulic conductivities; shallowing ETg extinction depths; stream incisions at or near ETg extinction depths; and, in some cases, discontinuous streams. Capture map bias tends to decrease in magnitude where combinations of model parameters result in more drawdown in the simultaneous pumping scenario (actual capture) than in capture interpreted from a capture map.

Capture map bias is sensitive to model parameters that significantly affect the transmissivity of a nonlinear groundwater system (i.e., aquifer hydraulic conductivity, saturated thickness). Transmissivity, as a factor in diffusivity, is a spatially controlling factor in the timing of changes in a system's state of dynamic equilibrium (Barlow and Leake 2012). Lower hydraulic conductivities increase the time for drawdowns to propagate to boundaries and increase the time for a system to return to a state of equilibrium (Bredehoeft et al. 1982). Capture bias tends to be greater in a lower hydraulic conductivity aquifer system. As flow becomes less restricted with increasing aquifer hydraulic conductivity, the delay in timing is diminished, thus reducing the capture map bias. However, when hydraulic conductivities are substantially increased, pumping wells will restrict the spatial extent of head-dependent processes (e.g., as represented with the MODFLOW SFR or EVT Packages) sooner and more extensively, thus reversing the behavior of capture bias.

Although aquifer hydraulic conductivity has a substantial effect on capture bias, streambed hydraulic conductivity does not. Ultimately, capture map bias arises from differences in drawdown associated with CMDC and actual capture. Though streambed hydraulic conductivity does affect quantitative capture, it does not affect the rate of drawdown in a system and thus does not contribute to capture map bias. Further, unconfined aquifers, simulated as convertible layers with nonlinear equations within MODFLOW, allow saturated thickness to vary with the position of the water table. This allows extensive pumping to result in large hydraulic gradients in the system (Niswonger et al. 2011). Because unconfined aquifers are represented with nonlinear equations that allow changing groundwater-level conditions, simulating these aquifer systems inevitably leads to capture bias using capture map approaches. Because capture map methods require the simulation of a pumping well, saturated thickness will predictably change near the well, thus changing transmissivity which in turn causes a nonlinear response.

Capture bias is also sensitive to well proximity to a stream. Capture bias is greater for wells pumping far from a stream than for wells closer to a stream. Generally, capture bias is larger when capture fractions are small, and vice

versa. That is, wells placed near a stream will derive more water from streamflow depletion than wells placed far from the same stream (Cooper and Rorabaugh 1963; Jenkins 1968; Peterson et al. 2008; Lackey et al. 2015). As a result, when supply is capture-dominated, CMDC is the same, or very nearly the same, as actual capture. Thus, total capture caused by pumping wells near a stream tends to have substantially lower capture map bias (often near zero) than wells farther from a stream. Because capture maps are increasingly used to conjunctively manage surface water and groundwater, water managers may use CMDC approach for nonlinear groundwater flow models more confidently in regions with low capture map bias, but limitation for capture map use may occur for some applications that result in higher capture map bias.

Conclusions

The effect a pumping well has on surface water (e.g., rivers) is of concern to water users and water managers—particularly where water is in short supply. Capture maps and capture fractions provide spatiotemporal information regarding capture by wells in an easily automated and interpreted format. As a result, capture maps are increasingly being used for conjunctive management of groundwater and surface-water resources. In much of the arid western United States nonlinear flow processes such as ET_g, drying streams, and unconfined aquifers need to be incorporated into groundwater flow models to adequately simulate flow processes. However, capture maps developed from nonlinear groundwater flow models may potentially limit the predictive accuracy of capture estimates for a given area. Understanding the behavior and magnitude of capture map bias associated with nonlinear groundwater flow models can guide water managers toward designing more realistic model simulations as the basis for capture maps.

Capture difference maps are a useful tool in understanding spatial and temporal variability of capture bias. Regions with large capture fraction differences are especially sensitive to pumping rate, and are indicative of greater potential capture map bias. Capture map bias generally increases as wells are placed farther from a source of capture (i.e., a stream and riparian ET_g zone). That is, when supply is capture-dominated with wells placed near a capture source, capture interpreted from a capture map is very nearly the same as actual capture. Thus, water managers may use capture derived from capture maps more confidently for some regions and maps may have greater limitations in other regions for conjunctive management of groundwater and surface-water resources. Capture difference maps may be used to select the appropriate spatial extent for a capture map by removing regions with capture differences greater than about 10%. Capture maps that are excessively limited by capture bias may be impractical and thus require individual model runs with existing well locations and pumping rates to determine capture.

Generally, capture bias associated with use of capture maps of arid regions derived from nonlinear groundwater flow models is sensitive to: aquifer hydraulic conductivity; ET_g extinction depth; depth of stream incision; discontinuous streams; pumping rate; and well proximity to sources of capture. Capture map bias is not sensitive to: stream representation (MODFLOW CHD vs. MODFLOW SFR Packages) for a connected stream; streambed hydraulic conductivity; specific yield; number of model layers; potential ET as specified by maximum ET_g rate; or grid discretization. Regions with changes in bias-sensitive parameters (i.e., stream incision, stream continuity) may require managers to consider updating capture maps and/or bias analyses.

Capture bias associated with nonlinear groundwater flow models can vary greatly depending on degree of model nonlinearity derived through model design and conceptualization. With increasing model nonlinearities, capture bias can interfere with the interpretation of capture map results. As capture bias is relatively easy to evaluate, the methods developed herein are recommended to assess the validity of capture maps created with nonlinear models for existing pumping distributions, particularly spatial validity for understanding capture map regions that may yield greater bias in interpretations.

Acknowledgments

This study is supported by the Nevada Division of Water Resources and the U.S. Geological Survey Cooperative Water Program. Stanley Leake, Leonard Konikow, Philip Gardner, Daniel Bright, and Michael Fienen of the U.S. Geological Survey and anonymous reviewers provided valuable feedback which greatly improved the manuscript. The authors would like to thank C.J. Mayers of the U.S. Geological Survey for developing the Python scripts used in this study and for his insight in automating many of the calculations and routines used to develop the methods described above. The authors also wish to thank Josh Lee of the U.S. Geological Survey for his assistance on the map figures.

Supporting Information

Additional supporting information may be found online in the Supporting Information section at the end of the article. Supporting Information is generally *not* peer reviewed.

Appendix S1. The archive for the hypothetical streamaquifer model described in this paper can be found at <http://dx.doi.org/doi:10.5066/F7639NN9>.

References

- Barlow, P.M., and S.A. Leake. 2012. Streamflow depletion by wells—Understanding and managing the effects of groundwater pumping on streamflow. U.S. Geological Survey Circular 1376. Reston, Virginia: USGS.
- Bredehoeft, J.D., S.S. Papadopoulos, and H.H. Cooper Jr.. 1982. Groundwater: The water budget myth. In *Scientific Basis of Water-Resource Management*, 51–57. Washington, D.C.: National Research Council (U.S.), Geophysical Study Committee.
- Cooper, H.H., and M.I. Rorabaugh. 1963. Ground-water movements and bank storage due to flood stages in surface streams. Water Supply Paper.
- Cosgrove, D.M., and G.S. Johnson. 2005. Aquifer management zones based on simulated surface-water response functions. *Journal of Water Resources Planning and Management* 131, no. 2: 89–100.
- Davids, J.C., and S.W. Mehl. 2014. Sustainable capture: Concepts for managing stream-aquifer systems. *Groundwater* 53: 851–858.
- Harbaugh, A.W. 2005. MODFLOW-2005, The U.S. Geological Survey modular ground-water model—The ground-water flow process. U.S. Geological Survey Techniques and Methods 6-A16. Reston, Virginia: USGS.
- Harbaugh, A.W., E.R. Banta, M.C. Hill, and M.G. McDonald. 2000. MODFLOW-2000, The U.S. Geological Survey modular ground-water model—User guide to modularization concepts and the ground-water flow process. U.S. Geological Survey Open-File Report 00-92.
- Jenkins, C.T. 1968. Computation of rate and volume of stream depletion by wells. U.S. Geological Survey Techniques of Water Resources Investigations, Book 4. Reston, Virginia: USGS.
- Konikow, L.F. 2014. Offsetting streamflow depletion from well pumpage by capture of evapotranspiration. In AGU 2014 Fall Meeting. San Francisco, CA.
- Konikow, L.F., and S.A. Leake. 2014. Depletion and capture: Revisiting ‘the source of water derived from wells’. *Groundwater* 52, no. Suppl 1: 100–111.
- Lackey, G., R. Neupauer, and J. Pitlick. 2015. Effects of streambed conductance on stream depletion. *Water* 7, no. 1: 271–287.
- Leake, S.A., D.R. Pool, and J.M. Leenhouts. 2008. Simulated effects of ground-water withdrawals and artificial recharge on discharge to streams, springs, and riparian vegetation in the Sierra Vista subwatershed of the Upper San Pedro Basin, southeastern Arizona. U.S. Geological Survey Scientific Investigations Report 2008-5207. Reston, Virginia: USGS.
- Leake, S.A., H.W. Reeves, and J.E. Dickinson. 2010. A sew capture fraction method to map how pumpage affects surface water flow. *Groundwater* 48, no. 5: 690–700.
- Niswonger, R.G., M. Ibaraki, and S. Panday. 2011. MODFLOWNWT. A Newton formulation for MODFLOW-2005. *U.S. Geological Survey Techniques and Methods* 6, no. A37: 44.
- Niswonger, R.G., and D.E. Prudic. 2005. Documentation of the streamflow-routing (SFR2) package to include unsaturated flow beneath streams—a modification to SFR1. U.S. Geological Survey Techniques and Methods 6-A13. Reston, Virginia: USGS.
- Peterson, S.M., J.S. Stanton, A.T. Saunders, and J.R. Bradley. 2008. Simulation of ground-water flow and effects of ground-water irrigation on base flow in the Elkhorn and Loup River Basins, Nebraska. U.S. Geological Survey Scientific Investigations Report 2008-5143. Reston, Virginia: USGS.
- Reilly, T.E., O.L. Franke, and G.D. Bennett. 1987. The principle of superposition and its application in groundwater hydraulics. U.S. Geological Survey Open-File Report 84-459.
- Stanton, J.S., S.M. Peterson, and M.N. Fioren. 2010. Simulation of groundwater flow and effects of groundwater irrigation on stream base flow in the Elkhorn and Loup River Basins, Nebraska, 1895-2055—Phase Two. U.S. Geological Survey Scientific Investigations Report 2010-5149.
- Theis, C.V. 1940. The source of water derived from wells: Essential factors controlling the response of an aquifer to development. *Civil Engineers* 10: 277–280.

Authors' Note

The authors do not have any conflicts of interest or financial disclosures to report.